Image fusion for enhanced forest structure assessment

J. W. ROBERTS*†, J.A.N. VAN AARDT‡, and F. B. AHMED§

†*Council for Scientific and Industrial Research, Natural Resources and the Environment, Ecosystems, Earth Observation, P.O. Box 320, Stellenbosch, 7600, South Africa

‡Council for Scientific and Industrial Research, Natural Resources and the Environment, Ecosystems, Earth Observation, P.O. Box 395, Pretoria, 0001, South Africa

§ University of Kwazulu-Natal, School of Environmental Sciences, King George V Avenue, Glenwood, Durban, 4041, South Africa

Abstract

This research explores the potential benefits of fusing active and passive medium resolution satellite-borne sensor data for forest structural assessment. Image fusion was applied as a means of retaining disparate data features relevant to modeling and mapping of forest structural attributes in even-aged (4-11 years) *Eucalyptus* plantations, located in the southern Kwazulu-Natal midlands of South Africa. Remote sensing data used in this research included the visible and near-infrared bands of the Advanced Spaceborne Thermal Emission and Reflection Radiometer (ASTER), as well as a fine beam (6.25 m resolution) Radarsat-1 image. Both data sets were collected during the spring of 2006 and fused using a modified discrete wavelet transformation. Spatially referenced forest inventory data were also collected during this time, with 122 plots enumerated in 38 plantation compartments. Empirical relationships (ordinary and multiple regression) were used to test whether fused data sources produced superior statistical models. Secondary objectives of the paper included exploring the roles of texture, derived from grey level co-occurrence matrices, and scale in terms of forest modelling at the plot and extended plot levels (Voroni diagrams). Results indicate that single bands from both the optical and SAR data sets were not adept at modeling both basal area and merchantable timber volume with adjusted R^2–values < 0.3. An optimized multiple regression approach (adjusted R^2) improved results based on mean, range, and standard deviation statistics when compared to single bands, but were still not suitable for operational forest applications (Basal Area = 0.55 & Volume = 0.59). No significant difference was found between fused and non-fused data sets, however optical and fused data sets produced superior models when compared to SAR results. Investigations into potential benefits of using textural indices and varied scales also returned inconclusive results. Findings indicate that the spatial resolutions of both sensors are inappropriate for plantation forest assessment. The frequency of the *C*-band Radarsat-1 image is for instance unable to penetrate the canopy and interact with the woody structures below canopy, leading to weak statistical models. The lack of variability in both the optical and SAR data lead to unconvincing results in the fused imagery, where in some cases the adjusted R^2 results were worse than the single data set approach. It was concluded that future research should focus on high spatial resolution optical and LiDAR data and the development of automated and semi-automated forest inventory procedures.

Keywords*: forest structure, image fusion, merchantable volume, basal area, Eucalyptus grandis*

1. Introduction

Sustainable forest management requires data that is spatially explicit, comprehensive, and geometrically accurate (Franklin 2001). Forest managers are constantly measuring and mapping forest health and timber resources within a sustainable management framework (Baskent and Keles

* Corresponding author. Email: wroberts@csir.co.za

2005) and accurate measurements allow the forest manager to describe and understand relationships that exist within the forest stand (Running *et al.* 1986). These relationships lead to an enhanced knowledge-base of the resources available, and place the forester in a position to make informed decisions regarding silviculture, harvesting, and stand rotation. The timber industry southern Africa is managed based on a short rotation scheme where single tree species are grown as part of a mono-culture agricultural crop (Owen 2000). The short rotation scheme used in South Africa requires an inventory program that constantly updates inventory databases with relevant information that is primarily used for the planning of silviculture and harvesting activities (Uys 2000). Collection of this information constitutes a time consuming manual process that requires a large amount of logistical and financial support. Increasing competition from international growers and decreasing profit margins have highlighted the need for streamlining forest management activities, in particular, the assessment of forest structure through inventory procedures. Remote sensing tools have long been identified as a means of streamlining this process and already play an important role in forest management (Norris-Rogers *et al.* 2006).

Forest stand structure characteristics are typically modelled using various statistical techniques (Rahman *et al.* 2005), whereby forest characteristics are measured during field campaigns and related to remotely sensed satellite data (Castro *et al.* 2003, Lu 2005). Relationships between the data and measured forest structure variables are often derived in the form of a statistical model, e.g.

$$FS = A*dn + B \quad (1)$$

where *FS* is the forest structure variable being analysed, A is the slope of the equation, *dn* is the digital number (either radiance or reflectance) of the satellite image, and B is the intercept. The objective is to derive an equation that explains most of the variance in the measured field data using remotely sensed imagery (Turner *et al.* 1999, Cohen *et al.* 2003, Foody *et al.* 2003), followed by extrapolation of such a relationship towards derivation of spatially explicit maps of the variable of interest (Lefsky *et al.* 1999, Zheng *et al.* 2004). Various authors have made use of empirical approaches using medium resolution satellite imagery (Aplin 2006)) with a spatial resolution of between 6 and 100 m for the quantification of inventory variables. The use of medium resolution imagery for this task relates to the synoptic scale view of these sensors with single scenes covering many hundreds of square kilometres and therefore resulting in the potential to inventory large forested areas with one scene.

Inventory variables have been quantified and mapped by various authors using several different approaches. Stand density (number of trees per unit area) and basal area in Madagascar were assessed using a combination of spectral channels and vegetation indices. The authors tested both linear regression and artificial neural networks (ANN) and found that the ANN approach produced strong significant relationships between spectral reflectance and basal area (r=0.79, p<0.01), while NDVI was significantly correlated to stem density (r=-0.69, p<0.01) (Ingram *et al.* 2005). Basal area has also been mapped using the K-nearest neighbours (k-NN) approach where field inventory data were used in combination with temporal Landsat scenes (Maselli *et al.* 2005). Results, quantified using the R^2 measure, ranged from 0.06 for single scenes to 0.68 for temporal data sets with the majority of R^2 values above 0.4. The k-NN approach is a popular method for forest inventory analysis, but is only suitable when a large number of field / training plots are available. Timber volume and biomass have also been quantified using remote sensing tools; Heiskanen (2006) used imagery acquired by the Advanced Spaceborne Thermal Emission and Reflection Radiometer (ASTER) to quantify above ground biomass recording good correlations between spectral reflectance ($r > 0.69$), vegetation indices ($r > 0.85$), and field measured biomass.

Researchers recently have used a combination of Moderate Resolution Imaging Spectroradiometer (MODIS) and ASTER data to estimate biomass (Muukkonen and Heiskanen 2007). The authors were able to use the ASTER data as an intermediary between field inventory data and coarse

resolution data by using regression equations derived from ASTER data (Muukkonen and Heiskanen 2005). This approach facilitated the development of a method by which inventory data and potentially carbon stocks could be monitored on a regular basis. Efficient empirical approaches to forest assessment using field measured inventory data have been developed (e.g., Rahman *et al.* 2005) and implemented in several studies with what appears to be suitable statistical accuracy. Turner *et al.* (1999) reported an adjusted R^2 of 0.74 for the modelling of leaf area index, while Foody *et al.* (2001) reported an adjusted R^2 value of 0.8 for assessment of above ground biomass. However, short rotation forestry of the type practiced in southern Africa, requires particularly accurate estimates of forest variables.

While the research presented seems to provide operational solutions to the industry there are, however, documented problems associated with the use of both passive and active medium resolution sensors. For instance, it has been shown that empirical models developed using optical data are site (Foody *et al.* 2003) and species (Zheng *et al.* 2004) specific. Empirical relationships, on the other hand, are stronger in successional forests ($R^2 > 0.7$) (Lu 2005) as opposed to mature forests ($R^2 < 0.5$), where saturation causes weak empirical models (Castro *et al.* 2003). Saturation has also been identified as a problem when using radar data, with radar frequency identified as being a primary contributing factor (*P-band:* 200 t/ha^{-1}; *L-band* 40 t/ha^{-1}; *C-band* 40 t/ha^{-1}) (Imhoff 1995, Ramsey 1999, Castel *et al.* 2002) along with the age and biomass of the forest in question (Austin *et al.* 2003). Recently it has been suggested that the fusion of multiple sensor systems may negate the impact of saturation and provide analysts and forest managers with accuracies suitable for operational planning and forest management (Holmgren and Thuresson 1998). Image fusion has been used operationally for military applications and has distinct potential benefits in forestry and sensor-web technology (Pohl and van Genderen 1998).

Optical systems use passive sensors that measure reflected radiance at different wavelengths of the electromagnetic magnetic spectrum (EM). Typically these data are collected in the visible, near- and shortwave infrared portions of the EM. Scientists are able to discern land cover features based on their spectral properties by combining these channels using a suitable color model (Hunt 1980). SAR sensors, on the other hand, illuminate off-nadir surfaces using short pulses of electromagnetic energy, part of which is reflected back to the sensor as backscatter (Bergen and Dobson 1999, Balzter 2001, Dobson 2000). The light energy used by radar sensors falls within the microwave portion of the EM with wavelengths ranging from 0.001-1 m (Bergen and Dobson 1999, Campbell 2002). It has been postulated that application-relevant details from each sensor can be combined into one data set which will result in the value of the combined data being more than the sum of the individual images (Ehlers 2005). This argument is based on the fact that both systems collect different types of information.

Tanaka *et al.* (1998) showed that by using optical and radar data, they were able to predict both species type and structural parameters with a high degree of accuracy. Moghaddam and Duncan (2001) and Moghaddam *et al.* (2002) have also reported positive results from the combined use of radar and optical sensors, particularly for the estimation of foliage mass and LAI. Furthermore, models developed were able to predict foliage biomass at levels that would not be possible if only one sensor was used (TM RMSE = 4.13 t/ha^{-1}, TM+SAR RMSE = 2.28 t/ha^{-1}). Magnusson and Fransson (2004) reported similar outcomes when assessing the accuracy of combined optical and radar data sets for stem volume estimates in Sweden. The authors reported that Root Mean Square Errors (RMSE) improved by up to 15% using regression techniques when compared to results derived from single sensor analysis. A study using an alternative method (*K*-NN; Nearest Neighbours) in the same area also reported significant improvements in the estimation of forest variables (Optical RMSE = 50 m^3/ha^{-1}, Optical+SAR = 37 m^3/ha^{-1}) (Holmstrom and Fransson 2003). They also found that optical data provided more robust estimates at lower stem volumes while the inverse was true for SAR, which lead to the result where the combination of both sensors

provided robust estimates throughout the age range (Optical RMSE = 66 m^3/ha^{-1}, SAR RMSE = 51.9 m^3/ha^{-1}, Optical+SAR = 38 m^3/ha^{-1}). The combined use of SAR and optical data has thus shown potential for forest inventory applications. However, it is not known whether image fusion will have the same impact in the southern African forestry industry where largely homogenous stands of mono-culture timber species are grown on relatively short rotation schedules.

This study investigated the use of optical remote sensing and synthetic aperture radar (SAR) systems for forest structural assessment in managed, even-aged, short rotation plantations. It also explored the potential benefits of using a combined optical / SAR data set for forest structural assessment. Empirical models were computed between remote sensing data and field enumerated inventory data to determine the applicability of both active and passive remote sensing tools. The enumerated data included basal area (*ba*) and merchantable volume (*mvl*). Independent variables included the individual SAR and optical bands as well as several fused data sets. A sub-theme of the paper sought to explore the influence of SAR texture (Haralick 1979, van der Sanden and Hoekman, 2005), particularly in the fused data sets. Mean and contrast gray-level co-occurrence matrices, derived from the SAR image, were also fused with the optical bands using a wavelet-based image transformation and fusion procedure. A second sub-theme of the paper explored the scale at which modeling was most successful. Typically, remote sensing data are extracted from the images based on the size of the plots. The argument is that this reflectance data should characterize the inventory data sampled in the field. Our research extended this concept through the use of Voroni diagrams derived from the centre of each field plot and the boundaries of each compartment. The above analysis was stratified into young (4-6 yrs) and mature (7-11 yrs) plots. The potential use of medium resolution satellite data for forest assessment holds many advantages for operational applications, given the synoptic scale view of the sensor. This characteristic provides a wide field of view and enables rapid assessment of large areas, thereby reducing both time and cost of management and inventory activities, while the standardized approaches could lead to more accurate structural information.

2. Materials and Methods

2.1 Study Area

The study was conducted in the Kwazulu-Natal province located in eastern South Africa. The sampled plantation stands are located approximately 50 km south of the town of Pietermaritzburg (figure 1). The area is known locally as the southern Natal midlands. Rainfall falls predominantly in the summer months with cold dry winters and warm wet summers. Mean annual rainfall ranges from 746-1100 mm (Schulze 1997) and is associated with either frontal systems originating from the south or from thunderstorms generated from convection activity. Temperatures range from high 20°C values in summer to below 10°C in the winter. Extreme temperature changes are a function of altitude and proximity to the warm Indian Ocean. Soils in the area are characterized by fine sandy clay and humic topsoils that are underlain by yellow or red apedal subsoils. The topography of the study area is flat with undulating hills and is classified by Schulze (1997) as being low mountains. Altitude ranges from 362 m amsl to over 1500 m amsl with an average altitude of approximately 874 m amsl.

Insert figure 1 here

2.2 Data sets

2.2.1 Inventory Data

Sampled plantation compartments were identified using a Geographical Information System maintained by a local timber company. These data are deemed to be highly accurate (1:15,000), is routinely updated and contains the attributes which were used to select compartments for enumeration. Attributes included the location of compartments, compartment size (>1ha), planting and felling dates (> 4 years old; not due for harvesting), and coppice status. The compartment selection was also restricted to three species, namely *Eucalyptus grandis*, *Eucalyptus nitens* and a clone, *Eucalyptus grandis* x *nitens*. These species were selected following consultation with industry partners, based on their economic importance to the industry. Only compartments between the ages of 4 and 11 years were selected, since it is assumed that 4 year old compartments had reached maturity and required no additional silvicultural activities. A maximum age of 11 was used as most stands have been felled at this age. Wherever possible, the selection of compartments was also influenced by the compartment site quality. A gradient of good, medium and poor site qualities, based on total available soil water content, were defined, resulting in a total of 38 compartments being sampled.

Recent aerial photographs were used in conjunction with commercial timber stock maps to identify potential sample plot locations prior to field enumeration. Plot locations were located in the field using a hand held Global Positioning System (GPS). Canopy entry points into the compartments were recorded with distance and bearing measurements collected for the plot centres relative to the entry points, thereby negating poor and inaccurate GPS reception under canopies. Distance and bearing measurements were digitised in a GIS and used to locate the centre of each sample plot. The number of plots per compartment was determined based on the size of the compartment; the total area of the sample plots was more than 5% of the total surface area of the compartment wherever possible, with at least two plots sampled regardless of compartment size. Fifteen meter fixed-radius plots were established once the plot centres had been identified. Inventory measurements collected during the field campaign included diameter at breast height (*dbh*), tree height (*tht*), and stems per hectare (*spha*). All trees with a *dbh* $\geq$ 5cm were measured within each plot while heights were measured for only a sub-sample of trees. Tree height was measured using a Vertex III hypsometer; trees were selected for height measurement based on their *dbh* with the full range of *dbh* values sampled. The number of stems per plot was used to determine *spha*. A total of 122 plots were sampled in 38 compartments. *Dbh* and *tht* were used to derive statistical relationships between tree diameter and height. Logarithmic regression was used to predict the heights of unsampled trees. The regression equations used returned statistically significant R^2 values > 0.8 at the plot and compartment levels. Tree height was modelled using these equations for each tree and measured *dbh*. Derived inventory variables were calculated using established methods and equations. Basal area was calculated for all trees within the plot using the following equation (Avery and Burkhart 1994).

$$BA_i = \pi r^2 \tag{1}$$

Where BA_i is the basal area and r is the radius calculated from *dbh*. It was possible to calculate *ba* per plot and hectare, since *spha* is known, which in turn was used to calculate merchantable tree volume using the following equation.

$$Vt = \frac{\left(\frac{\pi}{40000}\beta_0\right)}{\beta_1 + 1} DBH^2 HT \tag{2}$$

Where *Vt* is the volume of a single tree, and β_0 and β_1 are volume coefficients specific to plantation species used in this study. *DBH* and *HT* are the tree height and diameter at breast height, respectively. Table 1 shows the summary statistics of measured and derived variables.

Insert table 1 here

The plot level inventory data were digitised and stored in a GIS created using the GPS and distance and bearing measurements collected in the field. GPS data were accurate to ± 3 m with an acceptable error (± 5 m) associated with the distance and bearing measurements. The data stored in the GIS were then overlaid on the pre-processed remote sensing data and used for collocation and data extraction.

2.2.2 Remote Sensing Data

Passive (optical) data used in this study were captured by the Advanced Spaceborne Thermal Emission and Reflection Radiometer (ASTER) flying onboard the TERRA spacecraft. The sensor images the earth in a sun-synchronous orbit approximately 705 km above the surface of the earth. The sensor images in the visible, near-infrared, and shortwave infrared using three separate cameras with a temporal resolution of approximately 16 days, provided weather conditions allow for repeat measurements (Yamaguchi *et al.* 1998). RadarSAT-1 captured the synthetic aperture radar (SAR) scene. The imagery was collected on the 17th of October 2006 approximately one month before the ASTER scene (20th November 2006). RadarSAT-1 is a C-band synthetic aperture radar collecting data at various spatial resolutions and incidence angles. The data used in this study were fine-beam data (± 6.25 m) collected at an incidence angle of 47.703°. The C-Band sensor has a wavelength of 5.6 cm with a single polarization in the horizontal plane.

Pre-processing of the ASTER data began with the geometric correction of the level 1B data. Level 1B data are delivered as radiometrically calibrated and geometrically coregistered bands for all channels. Geometric correction was only applied to the three VNIR bands of interest. Orthorectification was undertaken using the ORTHOENGINE module of PCI Geomatica (Version 10.1). Ground control points (GCPs) were digitized from a 1:50 000 topographical map using water bodies and road intersections as points of interest (suitability of GCPs was determined using the root mean square error of the orthorectification). A 20 m digital elevation model (DEM), produced by the Chief Directorate of Surveys and Mapping (CDSM), was used to correct for terrain-induced error. GCP root mean square error (RMSE) was 3.85 m with the final accuracy of the orthorectification well within the accepted half pixel tolerance. The level 1B data were converted to atmospherically corrected reflectance following orthorectification. Atmospheric correction was undertaken using the Fast Line of Sight Analysis of Spectral Hypercubes (FLAASH) algorithm (Felde *et al*. 2003); no atmospheric data were available for the acquisition day so a standard mid-latitude summer atmospheric model was used in conjunction with a rural aerosol model.

RadarSAT-1 pre-processing was also undertaken using the ORTHOENGINE module of PCI Geomatica. The SAR data were delivered in Hierarchical Data Format (HDF), Georeferenced Fine Resolution (SGF) imagery (path orientated). GCPs used in the ASTER geometric correction were also employed to correct the SAR image. Twenty one GCPs were used, most of which were located at or near the corners of small lakes and farm dams, as these features were readily identifiable in the SAR image. The data were corrected and projected to a common coordinate system (Gauss Conformal, central meridian 31° East, WGS 84) using the CDSM DEM and the 21 SAR GCPs. The projection is known locally as LO31. Orthorecitifed accuracy of the SAR image was also within the half pixel accepted tolerance (RMSE = 2.8 m). The SAR image required substantial radiometric processing following orthorectification; terrain error was corrected by using a built in SAR model

with speckle suppression and a 7x7 Kuan filter (Zhenghao and Ko, 1994). The final image was converted to radar backscatter (sigma nought) and rescaled to 8 bit grayscale (0 – 255). Two grey-level co-occurrence measures were also computed (Mean and Contrast) to investigate the textural elements in SAR imagery, with both data sets included in the final analysis.

2.3 Image Fusion

It was found that no image-to-image registration was required following the pre-processing of both the ASTER and RadarSAT-1 imagery, since the corrected data sets were both within one pixel of each other. The selected image fusion procedure was a modified discrete wavelet transformation (*dwt*). The approach modifies the standard *dwt* approach through the combined use of the Intensity-Hue-Saturation transformation and the *dwt* approach. A hybrid image fusion procedure that incorporates the IHS transformation into a *dwt* fusion procedure was recently described by Amolins *et al*. (2007) and has been used in this study. The approach is as follows: (i) The RGB optical data set is converted to IHS colour space; (ii) the SAR image is stretched to match the Intensity image; (iii) a *dwt* is then performed on the SAR and Intensity images; (iv) following decomposition, the detail and approximation coefficients from the SAR and Intensity image are combined using a substitution approach; (v) once combined, an inverse IHS-to-RGB transformation is performed using the modified Intensity band with the result being the fused optical and SAR channel. A similar method for the integration of SAR and optical data, using a modified Brovey transformation in conjunction with the 'á trous' wavelet decomposition scheme has been used by Chibani (2007). The author reported promising results using both qualitative and quantitative assessment procedures. A modified wavelet fusion procedure has also been used by (Alparone *et al*. 2004). In that study, however, the authors modified the IHS transformation by using a generalized intensity modulation (GI) approach. The GI approach extends to the use of an arbitrary number of input multispectral bands and applies similar procedures to those mentioned above.

All authors cited here reported improved results when using a modified approach. Results from qualitative and quantitative test runs on the SAR and optical imagery fusion using a variety of procedures is reported elsewhere. The present analysis used the Amolins *et al.* (2007) approach. Each optical band was fused individually to each of the SAR images. This resulted in one backscatter scene and two GLCM textural scenes, after which the resulting bands, were stacked to create pseudo optical bands.

2.4 Analysis Methodology

Plot level inventory data, described above, were joined to the plot centres, after which plot area was calculated based on the slope of the plot (also recorded in field). These data formed the base data set used in the empirical modelling of forest structural attributes. The measured and derived field data constituted dependent variables, while remote sensing data used as explanatory or independent variables. Plot level remote sensing data were extracted for each plot within the GIS. Three distributional measures were extracted for each plot, namely mean, range, and standard deviation. These values were extracted from the remote sensing data on a band-by-band procedure for areas coincident with the field plot locations. The area covered by each plot varied due to slope differences and in some cases only 5 or 6 pixels were extracted. The scale of the study therefore was increased, with the goal of ensuring viable statistical variability and subsequent increased variable ranges for the independent variables. Voroni diagrams were constructed using plot centres, after which inventory data were assigned to the larger Voroni plots based on spatial association. Remote sensing data were subsequently extracted based on the area of the Voroni diagrams with the

mean, range, and standard deviation extracted for each Voroni plot. Figure 2 provides an overview of the different scales used to extract pixel values from the remote sensing data.

2.4.1 Model development and variable selection

Unfused and fused data sets were compared using regression-based statistical models. Plot- and Voroni plot level variable mean, range, and standard deviation were used in multiple regression models, while only the mean values were used in the simple linear regression models. Output statistics used to compare the models included R^2, adjusted R^2, and Root Mean Square Error (RMSE). Two important inventory variables were modeled, namely basal area and merchantable timber volume. Five data sets were used to predict both basal area and merchantable volume at varying scales for 98 plots and Voroni-plots, where each of these data sets consisted of three bands consisting of either optical, radar, or pseudo-optical bands (fused data sets). The individual bands were initially used to predict the inventory variables using OLS; however, it was evident that several plots / Voroni- plots represented significant outliers and compromised the OLS results. Cook's distance was used to identify and remove outliers (Cook 1977).

All input bands plus their distributional measures (range and standard deviation) were used to predict inventory measures using a multiple regression approach. Cook's distance once again was used to identify and remove outliers. Statistical procedures were implemented using the SAS 9.1 (SAS Institute Inc) statistical software package. The adjusted R^2 approach was selected above regular stepwise approaches as the procedure assess each and every combination of input variables and selects the best combination based on a measure (adjusted R^2), which penalizes models with a large number of input variables. It was argued that optimization of models based on a measure that produces the smallest number of variables with the highest adjusted R^2, would facilitate an accurate comparison of the goodness of fit for each approach. The influence of texture and age were also assessed by incorporating these as independent variables.

Insert figure 2 here

3. Results

3.1 Basal Area: Plot level

Table 2 provides an overview of the results from the plot level analyses. Individual optical bands exhibited little or no relationship with field enumerated *ba*, this is especially evident when all field plots were employed. Relationships improved when the data were stratified into age groups (4-6 years old and 7-11 years old), although improvement was not distinct. Established understanding of the relationship between tree canopies and spectra was observed with the near-IR bands returning considerably higher R^2 and adjusted R^2 values. The multiple regression results shown in figure 3A indicated that while the individual bands are not that adept at modelling field enumerated *ba*, they returned improved results when combined (including range and standard deviation statistics). Results from the 4-6 (solid line) and 7-11 (stippled line) age groups did not differ based on adjusted R^2 values. The second unfused data set included the SAR bands which incorporated the backscatter image (Kuan) and the two textural indices (GLCM_M & GLCM_C). Mirroring the optical data, individual bands returned weak linear relationships which resulted in only a slight improvement in the 4-6 age groups. Multiple regression results using the SAR bands and their distributional measures once again returned improved R^2 and adjusted R^2 values. It is noteworthy that the 7-11 year old group returned the highest indicator values when compared with both the 4-6 and "all-

ages" data sets. Multiple regressions also revealed that optical data lead to improved results over the SAR data in the younger stands (4-6 years), with the inverse being true in the older stands (7-11 years). The two textural indices derived from grey level co-occurrence matrices (Mean and Contrast) presented no improvement for modelling basal area than the original backscatter image. The fused data sets (Kuan, GLCM_M, and GLCM_C) returned similar patterns with no appreciable improvement in either R^2 or adjusted R^2 values. Once again individual bands from all three data sets returned weak to limited relationships with field enumerated *ba*. However, all fused data sets in the 7-11 age range resulted in notably higher R^2 or adjusted R^2 values than the younger stands.

3.2 Basal Area: Voroni level

Table 2 shows the results for the *ba* analyses using remote sensing data collected from the Voroni-plots. Individual bands returned poor results, with the near-IR band in the 7-11 year old age group returning the highest R^2 and adjusted R^2 of 0.32 and 0.30, respectively. Individual bands exhibited no discernable difference between the age groups, while the multiple regression models returned similar results to the plot level analyses, i.e., both multiple regression models returned statistically significant models (see figure 3B). The individual SAR bands also resulted in weak relationships, while the multiple regression models showed a minor improvement. A significant difference exists between the 4-6 and 7-11 year old age group when comparing the multiple regression results, with the latter returning improved statistics. The SAR data set exhibited similar results, although the goodness of fit statistics were distinctly lower than the optical data, implying that at this scale the optical data provide improved models when compared to SAR data. The fused data sets (Kuan, GLCM_M, GLCM_C) followed the pattern of superior models in the 7-11 year age groups with all three data sets returning multiple R^2 and adjusted R^2 results that were higher than those for 4-6 year old data sets. Multiple regression models were also inferior to their unfused counterparts, with only the Kuan Fusion data set returning results comparable to the optical imagery. The Voroni-plot results were generally similar to the plot level results, save for marginally higher RMSE values, which indicated that modelling based on Voroni-plots were less precise than those developed at the plot level.

Insert table 2 and figure 3 here

3.3 Volume: Plot level

Results for the statistical analyses of volume at the plot level are shown in table 3. Statistics shown for all age groups indicate that models derived from individual and multiple optical bands were not adept at modelling plot level timber volume. Results improve when the data set was subdivided into young (4-6 years old) and older (7-11 years old) plots. Individual bands were still not capable of modelling structural timber resources with multiple regression models returning statistically weak models (see figure 4A). Results for the age groups differed, with the model for the 4-6 year old data marginally better than the 7-11 year old data set. The individual SAR bands also failed to accurately explain field enumerated variance, with the two age groups once again resulting in slightly improved models. While the younger stands produced superior models when using optical data, the inverse was true for SAR imagery. R^2 and adjusted R^2 values were higher in the 7-11 year old plots than they were in the 4-6 year old plots. The relationships were positive and weak, although statistically significant. Results for the fused data sets (Figure 4) were only marginally superior to those already mentioned. Multiple regression models produced slightly better results, but were still deemed inaccurate. Data from the 4-6 and 7-11 age groups displayed similar characteristics, with individual bands returning improved goodness of fit statistics. Models in the older age group generally explained more ground level variance; this was especially true for the two textural data sets where recorded R^2 and adjusted R^2 values were well over 0.5. RMSE results shown in figure

4C and D reflect the goodness of fit statistics mentioned above - an interesting result was that while the models developed with the 7-11 year old data set return higher R^2 and adjusted R^2 values, the RMSE results in the 4-6 year old data set were in some cases lower than those reported for the 7-11 data sets. This indicated that while modelling plot level volume in the older stands produced superior models, they may not be that precise when compared to the younger stands.

3.4 Volume: Voroni level

Table 3 details the regression results from the Voroni level analysis. The optical data displayed similar trends to the plot level results. Individual bands, regardless of age, failed to produce models with R^2 and adjusted R^2 larger than 0.3. Their multiple regression models, graphed in figure 4, exhibited slightly improved models following optimization using the adjusted R^2 technique. A similar pattern emerged when comparing age groups, namely that multiple regression models produced using the 4-6 year old data set exhibited higher R^2 and adjusted R^2 values than the 7-11 year stands. The inverse was once again true for the SAR data; older plots produced significantly better models than the younger plots. The goodness of fit statistics for the 7-11 year old SAR model was not as high as the optical data. However, combining the two data sets through fusion procedures and using these data to model plot level volume returned interesting results. The fusion had a negative effect on the results in the younger age group (4-6 years old) where the Kuan, GLCM_M and GLCM_C all resulted in inferior models. Improvements following fusion were observed in the older stand data set, where R^2 and adjusted R^2 values increased from below 0.5 to above 0.6. The highest goodness of fit statistics resulted from the GLCM_M model, with R^2 and adjusted R^2 values of 0.62 and 0.54, respectively. Another pattern that re-emerged was that of the inverse relationship between R^2 and adjusted R^2 and Root Mean Square Error (figure 4 C&D). The pattern first observed in the plot level volume results also seemed prevalent in the Voroni level data, again calling into question the precision of the models using the fused data.

Insert table 3 and figure 4 here

3.5 Texture and Scale

A sub-theme of the study sought to explore the influence of SAR texture, particularly in the fused data sets. SAR backscatter imagery is sensitive to textural changes in the forest canopy and can be used as a surrogate for forest structure (Wulder *et al.* 1998). The derivation of two established textural indices, namely mean and contrast grey-level co-occurrence matrices (GLCM_M; GLCM_C) potentially could highlight textural features not already evident in the backscatter image (Podest and Saatchi, 2002). It was hypothesized that the additional textural information would enhance the predictive capability of the models. Figures 3 and 4 show that textural indices produced superior models only when plot level data were used as independent variables. The differences between the model statistics were small, with adjusted R^2 values of 0.29 to 0.54. An Analysis of Variance (ANOVA) procedure was used to determine if there was a statistically significant difference between predicted inventory variables using different textural "treatments". Tables 4 and 5 and figures 5 and 6 report the results of the ANOVA analysis. It is clear that there was no significant difference between the three textural "treatments".

The scale analysis was aimed at determining if the inclusion of additional remote sensing information, extracted from the Voroni diagram area, produced improved models when compared to plot level data. Modelling thus occurred at two different scales with the hypothesis being that the larger Voroni diagrams would include more variability than the plot level data and thus produce more robust empirical models. Results from the multiple regression analysis were used to compare the plot and Voroni level data (Figures 3 and 4). While differences in model accuracy and precision

were evident when comparing age groups, this did not extend to the plot and Voroni data sets. Adjusted R^2 and RMSE values were similar for both scales, which indicated that the inclusion of potentially increased variability by extending the plot size did not improve model accuracy or precision. For example, the optical data set (age 4 – 6) returned an adjusted R^2 of 0.41 at the plot level and 0.35 at the Voroni level, showing a decrease in model fitness. Root mean square error results were also inconclusive with no apparent trends towards either the plot or Voroni level. RMSE values for basal area modelling ranged from 1.6 m^2/ha to over 6 m^2/ha (Figure 3 C and D), but this variability was related more to the data set used than the scale of the analyses. Goodness of fit statistics for volume modelling were similar to those returned in the basal area analyses, with adjusted R^2 values ranging from 0.2 to just under 0.6. Once again this variability was related to the data set used as opposed to the scale of the study.

Insert table 4 and figure 5 here
Insert table 5 and figure 6 here

4. Discussion

4.1 Modelling of forest parameters

The modelling of forest inventory parameters (basal area and merchantable volume) was carried out using both optical and microwave (SAR) data. Spectral reflectance from the VNIR bands of the ASTER scene used in this study was not able to explain significant amounts of field enumerated variance. In most cases the near-IR bands provided marginally better results than the green and red bands. This is in contrast to results published by Muukkonen and Heiskanen (2005), who found that individual bands returned correlation coefficients well over 0.5 (the present study resulted in R^2 values < 0.3). The authors also found that the green band was most sensitive to volume, while this study contradicted these results with only the near-IR band returning satisfactory results. Contradictory results could be due to several factors; firstly, the Muukkonen and Heiskanen (2005) study was conducted in boreal forests where different species of different ages were studied while the present study investigated even-aged mono-cultures. The different crown morphologies and varying levels of canopy closure would contribute to differing results. Secondly, the present study only used ordinary and multiple least squares regression while the Finnish study made use of non-linear approaches, which may be more appropriate in managed plantation environments.

Results improved significantly when range and standard deviation statistics were added to the mean reflectance. Optimised multiple regression models returned somewhat improved results with adjusted R^2 values > 0.3, thereby explaining more variance in the field enumerated data. Even though multiple regression models returned improved results, they were disappointing when compared to those in the published literature. Foody *et al.* (2001) used artificial neural networks and multiple independent variables to model above ground biomass, explaining 80% variance in field enumerated data. Zheng *et al.* (2004) used multiple regressions and achieved an R^2 of 0.67 for both pine and hardwood species. Lu (2005) found significant differences between mature and successional forests reporting R^2 values of 0.50 and 0.76, respectively. The major difference between the present study and those cited above is that the present study occurs in plantation forests, while research in the case of Foody *et al.* (2001), Zheng *et al.* (2004), and Lu (2005) were conducted in natural forests where forest canopies display significantly more spectral variability, associated with structural variability. In contrast, plantation forests do not display as much canopy spectral variability, thereby making it more difficult to use reflectance from these canopies to explain below-canopy structural variability. The very same problem is evident when investigating the SAR results.

Individual backscatter and textural indices resulted in weak relationships with field enumerated data. However, when optimised multiple regression models were used, the data explained increasingly more variance than the individual bands. As expected the older data set (7-11) returned improved results when compared to the younger plots. Basal area adjusted R^2 improved from 0.21 to 0.52 when comparing models developed using 4-6 and 7-11 year old plots, respectively, with the same being evident at the Voroni scale. Volume models derived using the same independent variables displayed similar properties at both the plot and Voroni levels, which returned improved adjusted R^2 values when older plots were used (table 8). However, for volume estimations the RMSE (m^3/ha^{-1}) exhibited inverse properties, where values were smaller in the young plots. This indicated that goodness of fit statistics were not necessarily an indication of model precision.

Past studies have shown that saturation of the relationship between SAR backscatter is common with asymptotes, usually determined by the wavelength (Dobson *et al.* 1992, Rauste *et al.* 1994, Imhoff, 1995, Ramsey 1999, Fransson and Israelsson, 1999) and to some extent the polarisation (Van de Griend and Seyhan 1999, Santos *et al.* 2003). It proved impossible to determine when and if saturation occurred in this study - older plots (7-11 years old) returned higher adjusted R^2 values than the younger plots (4-6 years old), which is counter-intuitive to established relationships. On the other hand, one could argue that previous studies have been conducted in natural forests where canopy morphological variation reflects below-canopy structural variation and thereby facilitates increased explanation of variability by SAR backscatter. The SAR sensor data were possibly also unable to properly explain the plantation canopy variation, for reasons similar to those for the optical data. Low R^2 and adjusted R^2 values are also a function of wavelength (Paloscia *et al*. 1999); the RadarSAT-1 system uses a C-band HH sensor with a wavelength of approximately 5.6 cm. This relatively short wavelength, when compared to *L*- and *P*-band sensors (Dobson *et al*. 1992), rarely penetrates the canopy with most of the backscatter originating from the top of the canopy. This characteristic severely restricts the modelling of basal area and timber volume in plantation forests.

4.2 Original versus Fused data sets

The fusion of optical and SAR data is based on the premise that both data sets contain valuable information that, when combined, produce a model that is more robust than the sum of the input data sets. Results discussed above indicate that the individual data sets could not explain more than 50% of the ground level variance. Established understanding indicates that optical sensors should model lower biomass levels with more accuracy than the SAR data and that the inverse be true at higher biomass levels (Magnusson and Fransson 2004). As such the combined data sets should in theory predict forest structural attributes with a higher degree of accuracy throughout the age-biomass-volume range. Results presented above indicate that models developed using the fused data were not necessarily better than the optical data (figures 3 and 4). However, in most cases the fused data sets produced models that were comparable to the optical data and were consistently better than the SAR models. The only exception to this was the plot level basal area modelling, where the SAR data explained in excess of 50% of dependent variable variance. This result confirmed that the C-band data are not suitable for assessing forest structure and that it would be more appropriate to employ either an airborne or satellite platform collecting data in the *L*- or *P*-band frequency. Such data would provide more information regarding the variability of trunk size as opposed to the variability of the canopy structure.

The spatial resolutions of both sensors were also not adequate in terms of quantifying locational scale variability. Nugroho *et al.* (2002) used high resolution intensity, coherence, and interferometric images, as well as high resolution Ikonos imagery to develop a forest management system for quantifying the spatial structure of forest canopies in Indonesia. The authors were able to identify different hierarchy levels within the canopy using hierarchical classification techniques.

Classifications revealed that mature trees tend to clump together and that tree-crowns had a unique spatial structure. It is this unique spatial structure, identified using high resolution SAR and optical imagery that allowed the researchers to classify the canopy structure. Several studies have reported positive results when combining data from different sensors. For example Moghaddam *et al*. (2002) returned superior results when combining an interferometric model and Landsat TM data (developed using an airborne *C*-band sensor). Overall RMSE improved by a factor of two from 4.13 tons/ha (optical alone) to 2.28 tons/ha (both SAR and optical). Unfortunately, present results did not improve the RMSE, with fused data sets consistently returning similar results to that of the optical data.

4.3 Role of texture and scale

The textural sub-theme of this research sought to explore the question; "Is there a statistically significant difference between predictions of inventory variables based on different textural treatments?" The treatments described were in fact a backscatter image and two textural indices (Mean and Contrast), derived from grey level co-occurrence matrices (Kuplich *et al.* 2003). The results from the ANOVA analysis showed that the differences between different textural "treatments" were insignificant, with little difference within age groups and between scales. This is not surprising, given that it has already been established that *C*-band data are not suitable for modelling plantation forest variables. Podest and Saatchi (2002) enhanced a multi-scale classification using textural measures, while Kuplich *et al.* (2005), working in the Brazilian Amazon, found that the addition of GLCM contrast texture increased adjusted R^2 values from 0.74 to 0.82. Present research was not able to replicate the results of the above mentioned research, with predictions of both basal area and volume not achieving the desired increase in accuracy.

The second sub-theme of the paper explored the impact of the scale at which remote sensing data are extracted from imagery. The approach also attempted to mitigate any additional errors associated with the location of field plots. Several papers have indicated that errors in the location of plots due to mapping inaccuracies have led to lower overall model fitness. Patterson and Williams (2003) investigated the potential registration errors as they effect forest cover classification. The authors found that registration errors increased the variance of the estimator by between 4 and 434%. Halme and Tomppo (2001) also investigated errors associated with plot location error and found that using a multicriteria approach reduced pixel RMSE of total volume per hectare by up to 36%. Results presented in table 2 and 3 and figures 3 and 4 show that regardless of the scale at which data were extracted, no improvement in model accuracy was observed.

5. Conclusion

Management of forests in the 21st century will increasingly require the utilisation of either airborne or spaceborne remote sensing platforms. The cost and time associated with conducting a manual inventory of timber resources is fast becoming a challenge to sustainable forest management. Remote sensing approaches have been identified as potential tools that, if implemented correctly, could provide substantial benefits to the industry. This study explored the use of medium resolution satellite data for forest structural assessment. A brief literature review indicated that while single sensors may be appropriate for forest assessment, these sensors suffer under high biomass conditions with most established relationships saturating above a certain age and/or biomass. Further, image fusion was identified as a potential image processing tool that could mitigate problems associated with saturation and poor model performance. This paper explored, based on

previous research, the potential benefits of using several fused data sets to determine if forest inventory models improved when fused data sets were used. The paper also explored the potential impacts of texture and scale at which remote sensing data are extracted.

Principle findings indicated that medium resolution data (6-100 m spatial resolution) are able to explain a limited amount of the variance in enumerated inventory variables. However, this was only achievable with an optimised multiple regression model. Single bands and channels were not able to predict inventory variables and should be omitted from future efforts. Fused and unfused data sets exhibited no significant difference when comparing goodness of fit statistics. Given that the individual bands struggled to attain coefficient of determinations above 0.5, it is not surprising that fused data sets return similar results. A lack of spatial resolution, coupled to a microwave sensor frequency not suited to canopy penetration, are some of the reasons for the weak statistical models. It could be argued that errors in plot location could have contributed to the results. However, the scale analysis showed that results remained unsatisfactory even when a larger representative area was used. Textural analysis showed that texture, derived from a backscatter RadarSAT-1 image, contained limited additional information related to forest structure.

Results reported here were disappointing when compared to those in the published literature. R^2 and adjusted R^2 values were distinctly poorer than that of published papers in many cases. However, the type of forest being studied plays a central role in this outcome: The homogenous nature of the plantation canopy in this case did not contain sufficient variability, as related to below-canopy structural variability, for modelling purposes. Explanation of such variability requires a sensor with a higher spatial resolution than the 6.25 m (RadarSAT-1) and 15 m (ASTER) data sets used in this study. These sensors are thus not suitable for operational assessment of even–aged, homogenous, mono-culture plantation forests. Further research is required to test and assess various other data sources and approaches, which are cognisant of the inherent homogeneity of plantation forests. Possible alternative sensors include high resolution satellite imagery or aerial photography with a spatial resolution < 4 m. *P*- and *L*-band SAR sensors, combined with polarimetric data, also are recommended for these conditions.

Image fusion of LiDAR and high resolution optical sensors has shown promising results (Hudak *et al.* 2002, McCombs *et al.* 2003, Coops *et al*. 2004) and it is suggested that such an approach should be assessed in plantation forest conditions. However, LiDAR data have been criticised for being too expensive, thus future research also needs to develop cost effective, application-driven solutions towards producing accurate, precise, and spatially explicit maps of forest variables of interest.

6. Acknowledgements

The authors would like to thank Mondi Business Paper for allowing them access to the plantations used in this study. This study would not have been possible without funding from both the Council for Scientific and Industrial Research (CSIR; South Africa) and Mondi Business Paper. A number of anonymous reviewers have also provided constructive feedback during the preparation of this manuscript.

Reference:

ALPARONE, L., BARONTI, S., GARZELLI, A., and NENCINI, F., 2004, Landsat ETM+ and SAR image fusion based on generalized intensity Modulation. *IEEE Transactions Geoscience and Remote Sensing,* **42,** pp. 2832 – 2839.

AMOLINS, K., ZHANG, Y., and DARE, P., 2007, Wavelet based image fusion techniques – An introduction, review and comparison. *ISPRS Journal of Photogrammetry &*

Remote Sensing, **62,** pp. 249 – 263.

APLIN, P., 2006, On scales and dynamics in observing the environment. *International Journal of Remote Sensing,* **27,** pp. 2123 – 2140.

AUSTIN, J. M., MACKEY, B. G., and KIMBERLY, P. V. N., 2003, Estimating forest biomass using satellite radar: an exploratory study in a temperate Australian *Eucalyptus* forest. *Forest Ecology and Management,* **176,** pp. 575 – 583.

AVERY, T.E., and BURKHART, H.E., 1994, *Forest Measurements*, 4th Edition. McGraw-Hill, Boston, USA.

BALTZER, H., 2001, Forest mapping and monitoring with interferometric synthetic aperture radar (InSAR). *Progress in Physical Geography,* **25,** pp. 159 – 177.

BASKENT, E. Z., and KELES, S., 2005, Spatial forest planning: A review. *Ecological Modelling,* **188,** pp. 145 – 173.

BERGEN, K. M., and DOBSON, M. C., 1999, Integration of remotely sensed radar imagery in modelling and mapping of forest biomass and net primary production. *Ecological Modelling*, **122,** pp. 257 – 274.

CAMPBELL, J. B., 2002. *Introduction to remote sensing.* (New York, The Guilford Press)

CASTEL, T., GUERRA, F., CARAGLIO, Y., and HOULLIER, F., 2002, Retrieval biomass of a large Venezuelan pine plantation using JERS-1 SAR data. Analysis of forest structure impact on radar signature. *Remote Sensing of Environment,* **79,** pp. 30 – 41.

CASTRO, K. L., SANCHEZ-AZOFEIA, G. A., and RIVARD, B., 2003, Monitoring secondary tropical forests using space-borne data: implications for Central America. *International Journal of Remote Sensing,* **24,** pp. 1853 – 1894.

CHIBANI, Y., 2007, Integration of panchromatic and SAR features into multispectral SPOT images using the 'a tròus' wavelet decomposition. *International Journal of Remote Sensing,* **28,** pp. 2295 – 2307.

COHEN, W. B., MAIERSPERGER, T. K., GOWER, S. T., and TURNER, D. P., 2003, An improved strategy for regression of biophysical variables and Landsat ETM+ data. *Remote Sensing of Environment,* **84,** pp. 561 – 571.

COOK, R. D., 1977, Detection of Influential Observation in Linear Regression, *Technometrics,* **19,** pp. 15 – 18.

COOPS, N. C., WULDER, M. A., CULVENOR, D. S., and ST-ONGE, B., 2004, Comparison of forest attributes extracted from fine spatial resolution multispectral and LiDAR data. *Canadian Journal of Remote Sensing,* **30,** pp. 855 – 866.

DOBSON, M. C., 2000, Forest information form synthetic aperture radar. *Journal of Forestry,* **98,** pp. 41 – 43.

DOBSON, M. C., ULABY, F. T., LETOAN, T., BEAUDOIN, A., KASISCHKE, E. S., and CHRISTENSEN, N., 1992, Dependence of radar backscatter on coniferous forest biomass. *IEEE Transactions on Geoscience and Remote Sensing,* **30,** pp. 412 – 415.

EHLERS, M., 2005. Beyond Pansharpening: Advances in Data Fusion for Very High Resolution Remote Sensing Data. *Proceedings, ISPRS Workshop 'High-Resolution Earth Imaging for Geospatial Information',* Hanover, Germany.

FELDE, G. W., ANDERSON, G. P., ADLER-GOLDEN, S. M., MATTHEW, M. W., and BERK, A., 2003, Analysis of Hyperion Data with the FLAASH Atmospheric Correction Algorithm. Algorithms and Technologies for Multispectral, Hyperspectral, and Ultraspectral Imagery IX. *SPIE Aerosense Conference, Orlando*. 21-25 April 2003.

FOODY, G. M., CUTLER, M. E., MCMOROW, J., DIETER, P., TANGKI, H., BOYD, D. S., and DOUGLAS, I., 2001, Mapping the biomass of Bornean tropical rain forests from remotely sensed data. *Global Ecology and Biogeography,* **10,** pp. 107 – 120.

FOODY, G. M., BOYD, D. S., and CUTLER, M. E. J., 2003, Predictive relations of tropical forest biomass from Landsat Tm data and their transferability between regions. *Remote Sensing of Environment,* **85,** pp. 463 – 474.

FRANKLIN, S. E., 2001, *Remote Sensing for Sustainable Forest Management.* (Boca Ranton, Lewis Publishers).

FRANSSON, J. E. S., and ISRAELSSON, H., 1999, Estimation of stem volume in boreal forests using ERS-1 C- and JERS-1 L-band SAR data. *International Journal of Remote Sensing,* **20,** pp. 123 – 137

HALME, M, and TOMPPO, E., 2001, Improving the accuracy of Multisource forest inventory estimates by reducing plot location error – a multicriteria approach. *Remote Sensing of Environment,* **78,** pp. 321 – 327.

HARALICK, R. M., 1979, Statistical and Structural approaches to texture. *Proceedings of the IEEE,* **67,** pp. 786-804.

HEISKANEN, J., 2006, Estimating aboveground tree biomass and leaf area index in a mountain birch forest using ASTER satellite data. *International Journal of Remote Sensing,* **27,** pp. 1135 – 1158.

HOLMGREN, P., and THURESSON, T., 1998, Satellite remote sensing for forest planning: a review. *Scandinavian Journal of Forest Resources,* **13,** pp. 90-110

HOLMSTROM, H., and FRANSSON, J. E. S., 2003, Combining remotely sensed optical and radar data in *K*NN-estimation of forest variables. *Forest Science,* **49,** pp. 409 – 418.

HUDAK, A. T., CROOKSTON, N. L., EVANS, J. S., FALKOWSKI, M. J., SMITH, A. M. S., GESSELER, P. E., and MORGAN, P., 2006, Regression modelling and mapping of coniferous forest basal area and tree density from discrete-return lidar and multispectral satellite data. *Canadian Journal of Remote Sensing,* **32,** pp. 126 – 138.

HUNT, G. R., 1980, Electromagnetic Radiation: The Communication link in Remote Sensing In *Remote Sensing in Geology*. G. S. Siegel and A. R. Gillespie, (eds.), pp. 5 – 45 (New York, Wiley).

IMHOFF, M. L., 1995, Radar backscatter and biomass saturation: ramifications for global

biomass inventory. *IEEE Transactions on Geoscience and Remote Sensing,* **33,** pp. 511 – 518.

INGRAM, J. C., DAWSON, T. P., and WHITTAKER, R. J., 2005, Mapping tropical forest structure in southeastern Madagascar using remote sensing and artificial neural networks. *Remote Sensing of Environment,* **94,** pp. 491 – 507.

KUPLICH, T. M., CURRAN, P. J., and ATKINSON, P. M., 2003, Relating SAR image texture and backscatter to tropical forest biomass. *Proceedings of the IEEE,* **4,** pp. 2872 – 2874, 21 – 25 July 2003.

KUPLICH, T. M., CURRAN, P. J., and ATKINSON, P. M., 2005, Relating SAR image texture to the biomass of regenerating tropical forests. *International Journal of Remote Sensing,* **26,** pp. 4829 – 4854.

LEFSKY, M. A., COHEN, W. B., HUDAK, A., ACKER, S. A., and OHMANN, J. A., 1999., Integration of Lidar, Landsat ETM+ and Forest Inventory data for Regional Forest Mapping. *ISPRS Workshop: Mapping Forest Structure and Topography by Airborne and Spacebourne Lasers,* November 9 – 11, La Jolla CA.

LU, D. 2005. Aboveground biomass estimation using Landsat TM data in the Brazilian Amazon. *International Journal of Remote Sensing,* **26,** pp. 2509 – 2525.

MAGNUSSEN, M., and FRANSSON, J. E. S., 2004, Combining airborne CARABAS-II VHF SAR data and optical SPOT-4 satellite data for estimation of forest stem volume. *Canadian Journal of Remote Sensing,* **30,** pp. 661 – 670.

MASELLI, F., CHIRICI, G., BOTTAI, L., CORONA, P., and MARCHETTI, M., 2005, Estimation of Mediterranean forest attributes by the application of k-NN procedures to multitemporal Landsat ETM+ images. *International Journal of Remote Sensing,* **26,** pp. 3781 – 3796.

McCOMBS, J. W., ROBERTS, S. D., and EVANS, D. L., 2003, Influence of fusing LiDAR and multispectral imagery on remotely sensed estimates of stand density and mean tree height in a managed loblolly pine plantation. *Forest Science,* **49,** pp. 457 – 466.

MOGHADDAM, M., and DUNCAN, J. L., 2001, Estimating forest variables from fusion of SAR and TM data and analytical scattering and reflectance models. *Geoscience and Remote Sensing Symposium. 2001 IGARSS '01, 2001 IEEE International,* **2,** Pp 885-887.

MOGHADDAM, M., DUNCAN, J. L., and ACKER, S., 2002, Forest variable estimation from fusion of SAR and multispectral optical data. *IEEE Transactions on Geoscience and Remote Sensing,* **40,** pp. 2176 – 2187.

MUUKKONEN, P., and HEISKANEN, J., 2005, Estimating biomass for boreal forests using ASTER satellite data with standwise forest inventory data. *Remote Sensing of Environment,* **99,** pp. 434 – 447.

MUUKKONEN, P., and HEISKANEN, J., 2007, Biomass estimation over a large area based on standwise forest inventory data and ASTER and MODIS satellite data: A possibility to verify carbon inventories. *Remote Sensing of Environment,* **107,** pp. 617 –

624.

NORRIS-ROGERS, M., AHMED, F., and COPPIN, P., 2006, Satellite Imagery in Forest management in South Africa: Separating the weeds from the trees. *GIM International*, **21,** pp. 18 – 19.

NUGROHO, M., HOEKMAN, D. H., and DE KOK, R., 2002, Analysis of the forest spatial structure using SAR and Ikonos Data. *Presented at ForestSAT Symposium*, Heriot Watt University, Edinburgh, August 5 – 9, 2002. 10p.

OWEN, D. L., 2000. Trees, Forests and Plantations in Southern Africa. In *Southern African Forestry Handbook Vol 1*, D. L. Owen (ed.), pp. 1 – 6 (Pretoria: Southern African Institute of Forestry).

PALOSCIA, S., MACELLONI, G., PAMPALONI, P., and SIGISMONDI, S., 1999, The potential of *C*- and *L*-band SAR in estimating vegetation biomass: the ERS-1 and JERS-1 experiments. *IEEE Transactions on Geoscience and Remote Sensing,* **37,** pp. 2107 – 2110.

PATTERSON, P. L., and WILLIAMS, M. S., 2003. Effects of Registration Errors between Remotely Sensed and Ground Data on Estimators of Forest Area. *Forest Science,* **49,** pp. 110 – 118.

PODEST, E., and SAATCHI, S., 2002, Application of multiscale texture in classifying JERS-1 radar data over tropical vegetation. *International Journal of Remote Sensing,* **23,** pp. 1487 – 1506.

POHL, C., and VAN GENDEREN, J. L., 1998, Multisensor image fusion in remote sensing: concepts, methods and applications. *International Journal of Remote Sensing,* **19,** pp. 823 – 854.

RAHMAN, M. N., CSAPLOVICS, E., and KOCH, B., 2005, An efficient strategy for extracting forest biomass information from satellite sensor data. *International Journal of Remote Sensing,* **26,** pp. 1511 – 1519.

RAMSEY, E. J., 1999, Radar remote sensing of wetlands. In: *Remote sensing change detection: environmental monitoring methods and applications,* R. S. Lunetta and C. D. Elvidge (eds.), pp. 211 – 243 (Taylor & Francis, London).

RAUSTE, Y., HAME, T., PULLIAINEN, J., HEISKA, K., and HALLIKAINEN, M., 1994, Radar-based forest biomass estimation. *International Journal of Remote Sensing,* **15,** pp. 2797 – 2808.

RUNNING, S. W., PETERSON, D. L., SPANNER, M. A., and TEUBER, K. B., 1986, Remote Sensing of coniferous forest leaf area. *Ecology,* **67,** pp. 273 – 276.

SANTOS, J. R., FREITAS, C. C., ARAUJO, L. S., DUTRA, L. V., MURA, J. C., GAMA, F. F., SOLER, L. S., and SANT'ANNA, S. J. S., 2003, Airborne P-band SAR applied to the aboveground biomass studies in the Brazilian tropical rainforest. *Remote Sensing of Environment,* **87,** pp. 482 – 493.

SCHULZE, R. E., 1997, *South African Atlas of Agrohydrology and –Climatology.* Water

Research Commission, Pretoria, Report TT82/96

TANAKA, S., SUGIMURA, T., SENOO, T., and NISHI, T., 1998, Forest stand structure analysis in Fuji area with OPS and SAR Data. *Advances in Space Research,* **22,** pp. 685 – 688.

TURNER, D. P., COHEN, W. B., KENNEDY, R. E., FASSNACHT, K. S., and BRIGGS, J. M., 1999. Relationships between Leaf Area Index and Landsat TM Spectral Vegetation Indices across three Temperate Zone Sites. *Remote Sensing of Environment*, **70,** pp. 52 – 68.

UYS, H. J. E. 2000. Timber Plantation Management. In *Southern African Forestry Handbook Vol 1,* D. L. Owen (ed) pp. 161 – 165 (Pretoria: Southern African Institute of Forestry).

VAN de GRIEND, A. A., and SEYHAN, E., 1999, Multi-temporal analysis of ERS-1 and EMISAR C band VV backscattering properties of forest and lake surfaces in the NOPEX region. *Agricultural and Forest Meteorology,* **99,** pp. 363 – 374.

Van Der SANDEN, J. J., and HOEKMAN, D. H., 2005, Review of relationships between grey-tone co-occurrence, semivariance, and autocorrelation based image texture analysis approaches. *Canadian Journal of Remote Sensing,* **31,** pp. 207 – 213.

WULDER, M. A., LE DREW, E. F., FRANKLIN, S. E., and LAVIGNE, M. B., 1997, Estimation of Northern Deciduous and Mixed Wood Forest Leaf Area Index. *Remote Sensing of Environment*, **64,** pp. 64 – 76.

YAMAGUCHI, Y., KAHLE, A. B., TSU, H., KAWAKAMI, T., and PNIEL, M., 1998, Overview of Advanced Spaceborne Thermal Emission and Reflection Radiometer (ASTER). *IEEE Transactions on Geoscience and Remote Sensing*, **36,** pp. 1062 − 1071.

ZHENG, D., RADEMACHER, J., CHEN, J., CROW, T., BREESE, M., LE MOINE, J., and RYU, S., 2004, Estimating aboveground biomass using Landsat 7 ETM+ data across a managed landscape in northern Wisconsin, USA. *Remote Sensing of Environment,* **93,** pp. 402 – 411.

ZHENGHAO, S., and FUNG, K. B., 1994, A Comparison of Digital Speckle Filters. *Proceedings of IGARSS*, August 8-12, 1994, pp. 2129-2133.

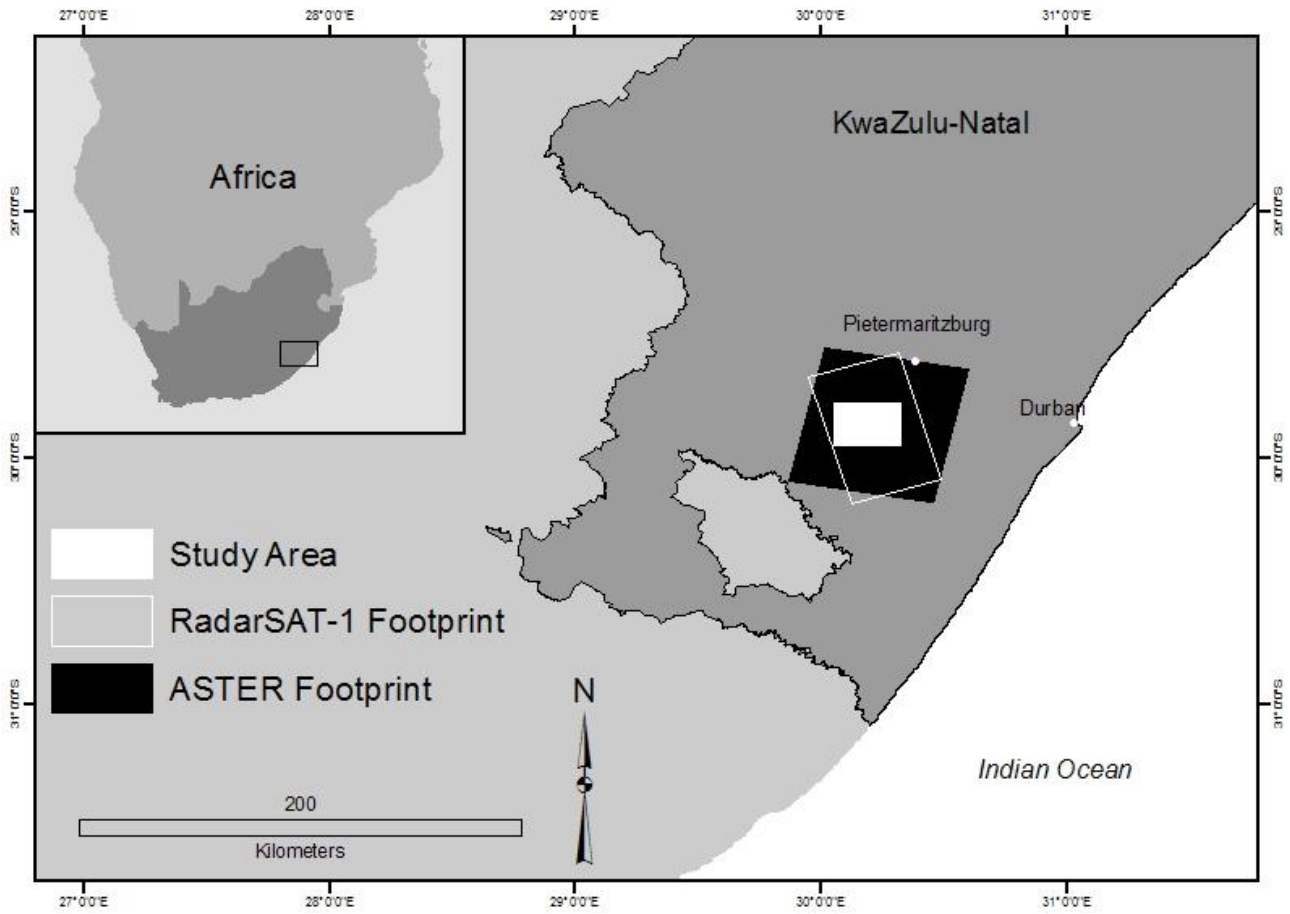

Figure 1 Location of study area

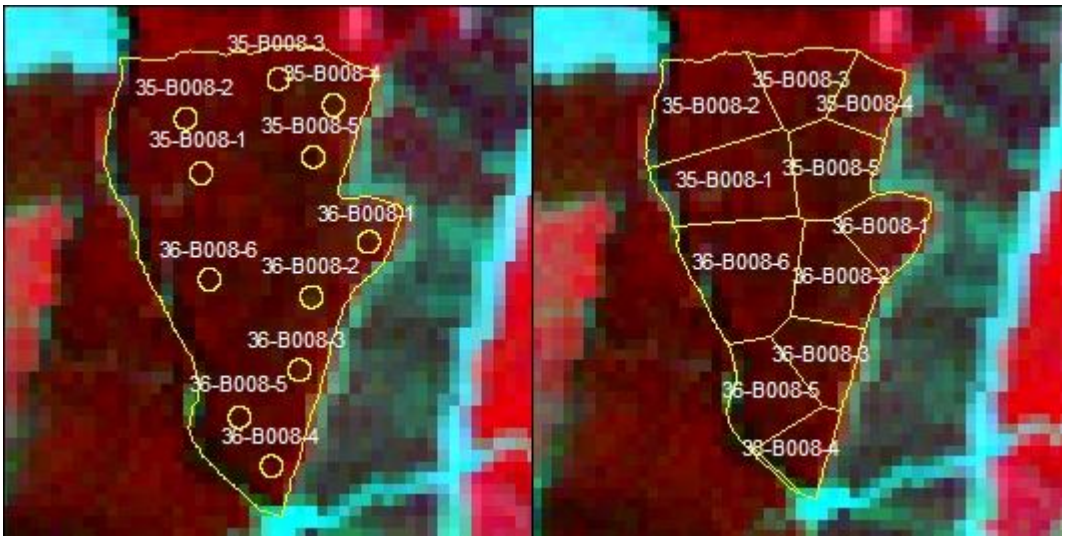

Figure 2 Plot (left) and Voroni (right) level data extraction

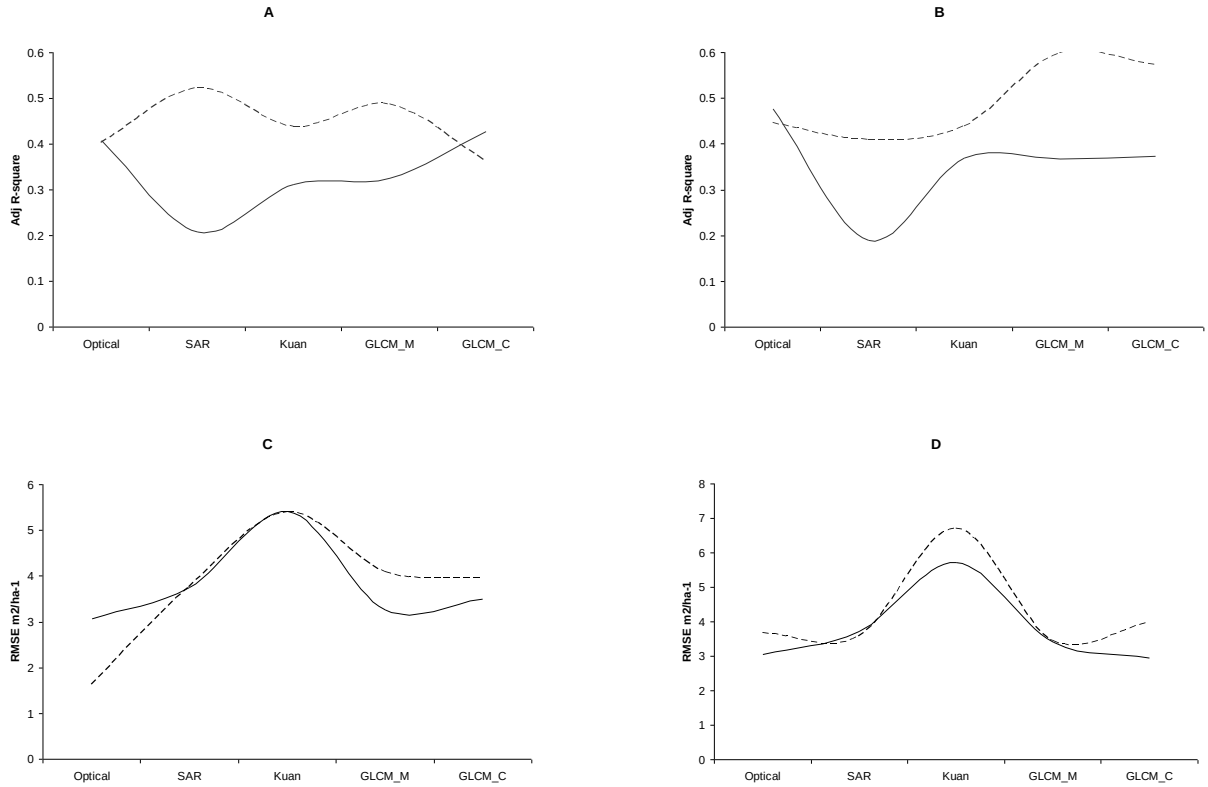

Figure 3 Results from *ba* optimized multiple regression models (A. Plot level Adj-R^2, B. Voroni level Adj-R^2, C. Plot level RMSE, D. Voroni level RMSE) – solid line: 4-6 yrs, stippled line 7-11 yrs.

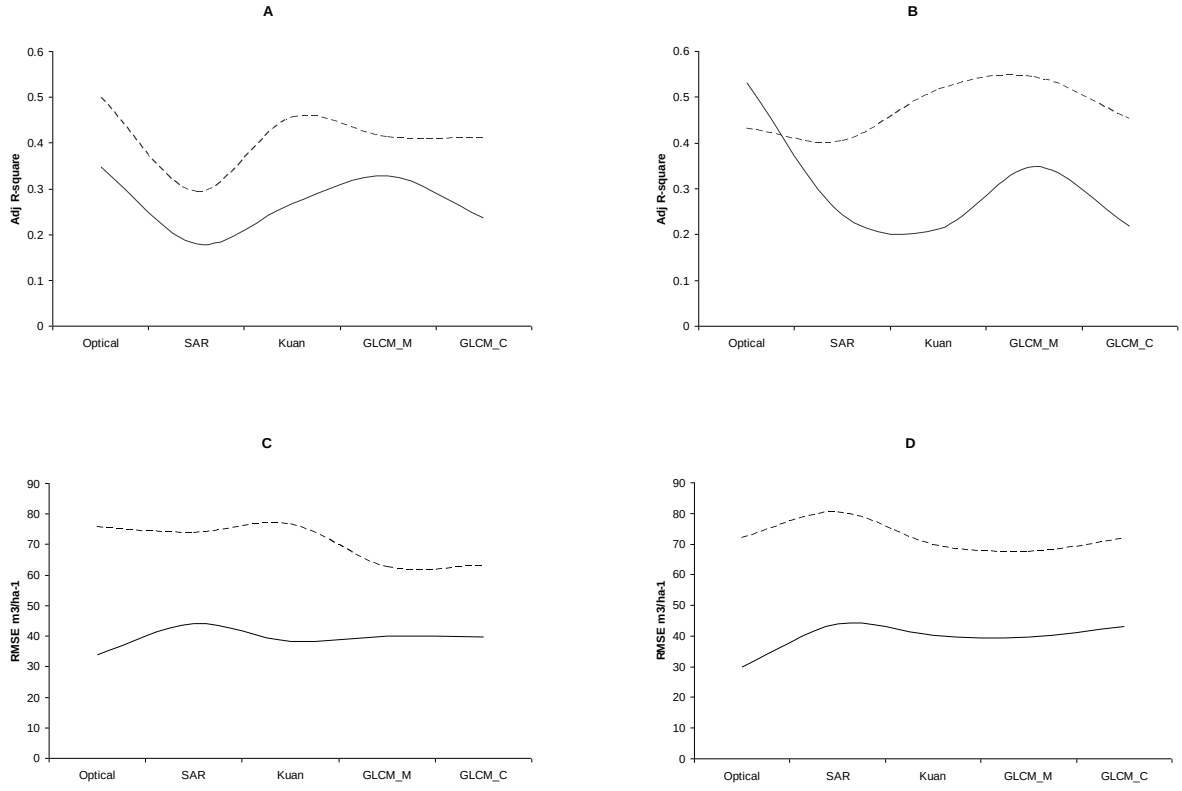

Figure 4 Results from *mvl* optimized multiple regression models (A. Plot level Adj-R^2, B. Voroni level Adj-R^2, C. Plot level RMSE, D. Voroni level RMSE) – solid line: 4-6 yrs, stippled line 7-11 yrs.

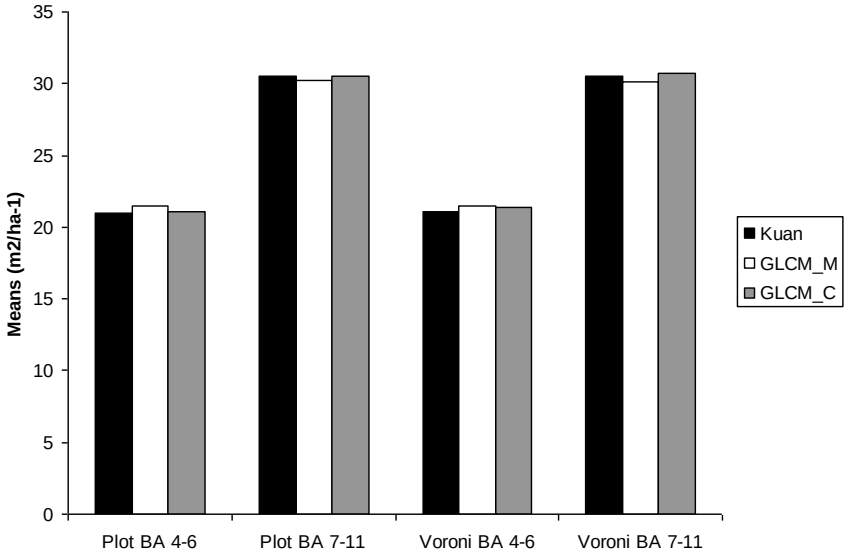

Figure 5 Predicted Basal Area Means for Textural indices (stratified according to scale and age)

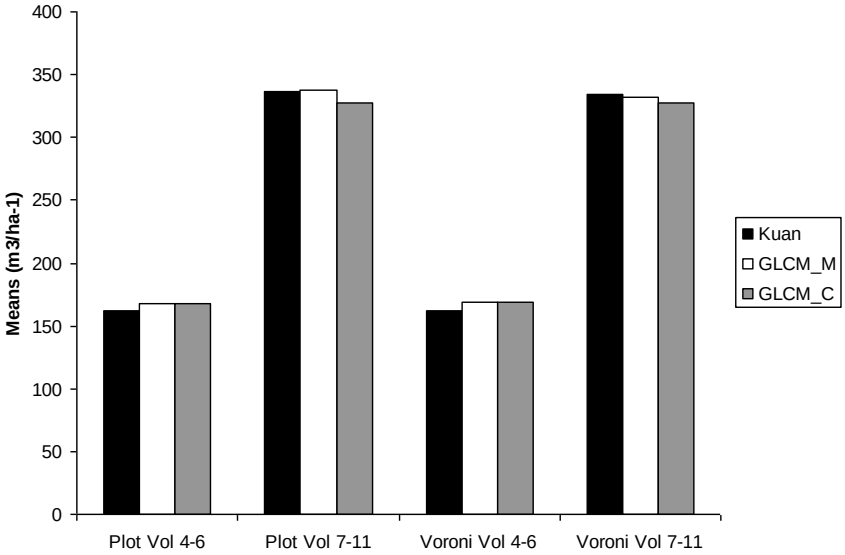

Figure 6 Predicted Volume Means for Textural indices (stratified according to scale and age)

Table 1 Summary statistics from enumerated inventory data: Basal Area and Merchantable Volume

Parameter	*Basal area of individual trees (m^2)*	*Plot level basal area per hectare (m^2)*	*Compartment level basal area per hectare (m^2)*
Minimum	0.00196- 0.0132	14.5	16.6
Maximum	0.02546-0.14528	48.1	38.3
Mean	0.0124-0.07087	26.6	26.9
Standard deviation	0.00514-0.03771	6.9	6.4
%CV	27.9-74.3	25.9	23.6
Parameter	*Volume of individual trees (m^3)*	*Volume per hectare (m^3)*	*Compartment level volume per hectare (m^3)*
Minimum	0.01-0.11	98.33	108.38
Maximum	0.19-2.63	746.73	584.25
Mean	0.08-1.16	259.95	268.38
Standard deviation	0.04-0.70	119.40	117.34

Table 2 Summary statistics for single band OLS regression – *Basal Area* (only optical and SAR reported)

Data set		4-6 years		7-11 years		All Ages	
	Band	**R^2**	**Adj R^2**	**R^2**	**Adj R^2**	**R^2**	**Adj R^2**
Optical (plot)	Green	.0572	.0372	.0328	.0092	.0640	.0531
	Red	.1522	.1334	.0670	.0458	.0861	.0760
	NIR	.1605	.1423	.2080	.1900	.0006	-.0102
SAR (plot)	Kuan	.2014	.1298	.0003	-.0235	.0529	.0425
	GLCM_M	.1783	.1596	.0007	-.0231	.0474	.0369
	GLCM_C	.1792	.1606	.0198	-.0030	.0119	.0012
Optical (voroni)	Green	.10060	.08110	.03040	.00780	.01920	.00840
	Red	.03690	.01960	.07490	.05340	.06480	.05440
	NIR	.10570	.08530	.28260	.26630	.01800	.00750
SAR (voroni)	Kuan	.02380	.00260	.01040	-.01210	.00030	-.01040
	GLCM_M	.01130	-.01020	.00930	-.01320	.00120	-.00950
	GLCM_C	.04050	.01920	.04490	.02270	.00370	-.00700

Table 3 Summary statistics for single band OLS regression – *Merchantable Volume* (only optical and SAR reported)

Data set		4-6 years		7-11 years		All Ages	
	Band	R^2	Adj R^2	R^2	Adj R^2	R^2	Adj R^2
Optical (plot)	Green	.07500	.05530	.06440	.04160	.05110	.03990
	Red	.03100	.00950	.15370	.13360	.06640	.05590
	NIR	.27050	.25460	.24370	.22610	.00080	-.01050
SAR (plot)	Kuan	.16040	.14170	.01390	-.00900	.06040	.05010
	GLCM_M	.15620	.13750	.03010	.00810	.03800	.02740
	GLCM_C	.00560	-.01510	.00910	-.01390	.01910	.00830
Optical (voroni)	Green	.10710	.08770	.03240	.00940	.00030	-.01400
	Red	.01930	-.00110	.13910	.11950	.02630	.01560
	NIR	.09830	.07780	.31570	.30010	.01990	.00920
SAR (voroni)	Kuan	.09200	.07180	.06270	.04090	.00000	-.01070
	GLCM_M	.09450	.07440	.06320	.04140	.01360	.00290
	GLCM_C	.02600	.00440	.10150	.08110	.01780	.00710

Table 4 Anova Results for Basal Area

Data	*F*-test	*p* value
Plot BA 4-6	0.36	0.69820
Plot BA 7-11	0.06	0.91390
Voroni BA 4-6	0.43	0.65150
Voroni BA 7-11	0.2	0.81630

Table 5 Anova results for Volume

Data	*F*-test	*p* value
Plot Vol 4-6	0.360573	0.69790
Plot Vol 7-11	0.19	0.82760
Voroni Vol 4-6	0.65	0.52290
Voroni Vol 7-11	0.067541	0.93470